



# Microstructure and Wear Performance of Arc Sprayed Fe-FeB-WC Coatings

Ding-Yong He, Bin-You Fu, Jian-Min Jiang, and Xiao-Yan Li

(Submitted May 11, 2008; in revised form September 13, 2008)

Two Fe-FeB-WC coatings were deposited on the Q235 steel substrate by arc spraying. The microstructure and the abrasive wear performance of the coatings were characterized by x-ray diffraction (XRD) and scanning electron microscope (SEM). The wear mechanisms of the coatings were examined. It was found that Fe-Cr alloy and Fe<sub>2</sub>B are present in the coating as the main phases. The results showed that adding hard particle powders could obviously increase the hardness and wear resistance of the coatings. The average microhardness of the coatings was about 870 to 920 HV<sub>0.1</sub>. The coatings exhibited excellent abrasive wear resistance, being 3.3 to 4.8 times higher than that of arc sprayed 3Cr13 coating.

**Keywords** abrasive wear resistance, arc spraying, Fe-FeB-WC coating

## 1. Introduction

Thermally spraying cermet coatings have emerged as a viable solution for a wide range of wear-resistance applications to improve the service life of machine components, due to their high hardness and good wear resistance (Ref 1). In order to enhance the wear resistance of many types of engineering components, WC, TiC, and Cr<sub>3</sub>C<sub>2</sub> particulates were commonly used as hard phases in the cermet. The wear resistance of FeNiCrB coatings, especially for abrasive wear, can be greatly increased by adding refractory carbides into the FeNiCrB matrix. Compared with cermet systems involving other carbides, the coatings containing WC are superior in hardness and wear resistance. WC coupled with Co, CoNi, Ni, or FeNiCrB matrix has been the preferred material for industrial applications used to reduce wear because of the combined effect of the hardness of carbides and toughness of the metal matrix (Ref 2). Hence, many research efforts have been made to

prepare the cermet coatings containing WC by different methods (Ref 3-10), including high-velocity oxyfuel (HVOF), plasma spraying (PS), and detonation gun spraying (DGS). Although industrial applications of these methods, especially HVOF, have become very popular because of the excellent wear performance of the resultant coating, arc spraying of wear-resistant coatings has been widely used for many industrial applications where good wear and corrosion resistance are highly required. The major advantages of arc spraying are low cost, high efficiency, and simple operation.

In order to improve the wear performance of arc sprayed coating, one possible solution is to add wear-resistant hard particles into the arc sprayed metallic alloy matrix. The development of the cored wire makes it possible to deposit hard phase containing cermet coating by arc spraying. In this study, cobalt-coated tungsten carbide (WC/12Co), nickel-coated tungsten carbide (WC/12Ni), and FeB alloy powders were used as fillers in the cored wire to produce Fe-FeB-WC composite coatings. However, the previous study showed that it was difficult to deposit a dense coating. In this paper, Ni powder was added in the filler materials to modify deposition behavior and coating microstructure. The microstructure and phase compositions of the coatings were investigated. The wear performance and mechanisms of the coatings were also investigated.

## 2. Experimental

Cored wire with a diameter of 2.0 mm was used to produce Fe-FeB-WC coatings. The sheath of the cored wire was 304L stainless steel. FeB (FeB<sub>18</sub>C<sub>0.5</sub>-A: 81.5% Fe, 18.0% B, 0.5% C; 150-250 μm, crushed; Liaoyang International Boron Alloys Co., Ltd. (LIB), China), WC/12Co (KF-60: 88% WC, 12% Co; 15-45 μm, agglomerated and sintered; Beijing General Research Institute of Mining & Metallurgy, China), and WC/12Ni (KF-60-1: 88% WC, 12% Ni; 15-45 μm, agglomerated and sintered;

This article is an invited paper selected from presentations at the 2008 International Thermal Spray Conference and has been expanded from the original presentation. It is simultaneously published in *Thermal Spray Crossing Borders, Proceedings of the 2008 International Thermal Spray Conference*, Maastricht, The Netherlands, June 2-4, 2008, Basil R. Marple, Margaret M. Hyland, Yuk-Chiu Lau, Chang-Jiu Li, Rogerio S. Lima, and Ghislain Montavon, Ed., ASM International, Materials Park, OH, 2008.

Ding-Yong He, Bin-You Fu, Jian-Min Jiang, and Xiao-Yan Li, College of Materials Science and Engineering, Beijing University of Technology, Beijing 100124, China. Contact e-mail: dyhe@bjut.edu.cn.

**Table 1** Composition of the filler materials

Coatings	Element, wt. %						
	Fe	Cr	Ni	B	W	Co	C
W1	70.12	12.67	7.14	4.05	5.07	0.72	0.23
W2	70.12	12.67	7.86	4.05	5.07	...	0.23

Beijing General Research Institute of Mining & Metallurgy, China) thermal spray powders were employed as the filler materials in the cored wire. The mass ratio of the 304L sheath to filler powders inside the sheath was 7:3. The coatings were sprayed onto degreased and grit-blasted Q235 steel substrates ( $56 \times 25 \times 5 \text{ mm}^3$ ) using two cored wires by arc spraying system (JZY-250, Beijing Jiazhiyuan Scientific & Trading Co., Ltd., China) under the optimized spray parameters. The parameters were: arc voltage, 32 V; arc current, 180 A; air pressure, 0.55 MPa; spray distance, 100 mm. Two coatings were deposited on Q235 steel, coatings W1 and W2. The thickness of both coatings was approximately 1.0 mm. The nominal composition of the coatings is listed in Table 1.

The microhardness of the coatings was measured using a microVickers hardness tester (MicroMet 1, Buehler). The measurements were carried out on the midplane of coating cross section with a 100 g load and 15 s dwell time. A given microhardness value was an average of 10 measurements.

The abrasive wear test was carried out using a modified wet sand rubber wheel (Model MLS-225, Zhangjiakou Chengxin Balance Testing Machineries Company, China). The specimen dimensions were  $57 \times 25 \times 6 \text{ mm}^3$ , and the coatings in a thickness of 1.0 mm were used. The silica in a sharp, angular morphology was used as an abrasive and was sieved into a particle size range of 224 to 355  $\mu\text{m}$  prior to the test. A load of 100 N was applied on the contact surface between the coating and the rubber wheel, and the rubber wheel peripheral speed was 240 rpm. The specimen was immersed in the abrasive mortar with the weight ratio of  $W_{\text{silica}}:W_{\text{water}} = 3:2$ . The tests were performed for a set number of revolutions with a preabrading of 1000 cycles and a refining abrading of 2000 cycles. The specimens were cleaned ultrasonically in the acetone bath for 3 to 5 min before and after the experiment. The weight loss of the specimen before and after abrasion was measured by a 0.1 mg BS224S electronic balance. An arc sprayed 3Cr13 coating was also deposited for comparison of the relative wear resistance of the hard phase contained coatings. The relative wear resistance ( $\sigma$ ) of the coatings was calculated using:

$$\sigma = \frac{m_{3\text{Cr}13}}{m_{\text{Coating}}} \quad (\text{Eq 1})$$

where  $m_{3\text{Cr}13}$  and  $m_{\text{Coating}}$  represent the wear mass loss of 3Cr13 coating and W1 or W2 coatings, respectively.

After abrasive wear test, a square specimen of  $5 \times 5 \text{ mm}^2$  was cut from the central part of the abrasive track. The wear track was examined by a FEI Quanta 200 FEG scanning electron microscopy (SEM) under the

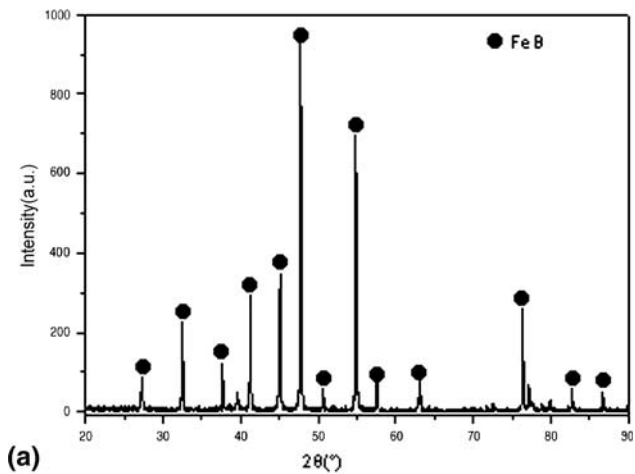
secondary electron (SE) images model. Composition analysis was also performed in the SEM by using a Noran energy-dispersive x-ray analysis (EDX) system, with a thin-window detector capable of analyzing elements with atomic number down to carbon. Cross-section microstructures of the coatings were observed by an optical microscope. The phases of the coatings were characterized by the x-ray diffraction (XRD) (D8 ADVANCE, BRUKER/AKS, Germany) using Cu  $K\alpha$  target at 40 kV and 20 mA. The porosity of the coatings was evaluated through image analysis of cross-sectional microstructure of the coatings. A total of 10 pictures of each coating were taken by an optical microscope at a magnification of 200 $\times$  to evaluate the average porosity levels.

### 3. Results

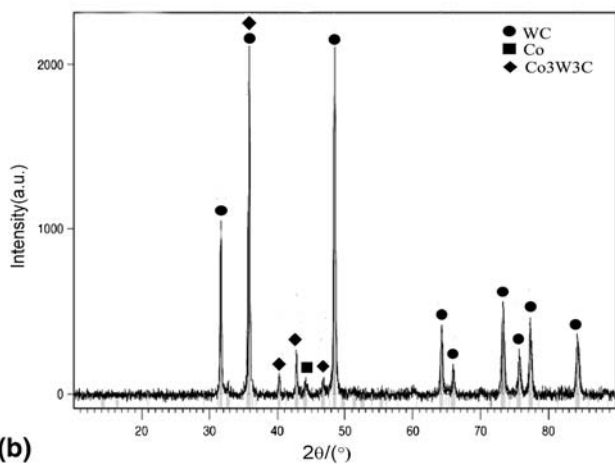
#### 3.1 Microstructural Characterization

The x-ray diffraction patterns of feedstock powders used as the fillers are shown in Fig. 1. In WC/12Co powder, WC, Co, and  $\text{Co}_3\text{W}_3\text{C}$  were detected, while in WC/12Ni powder, only WC phase was detected. Only FeB phase was detected in FeB powder. X-ray diffraction patterns of the coatings W1 and W2 are shown in Fig. 2. From the patterns, both coatings were mainly composed of Fe-Cr alloy with a fraction of  $\text{Fe}_2\text{B}$  and  $\text{Fe}_3\text{O}_4$ , and the broadening of the peak was observed. Probably the matrix material was presented in amorphous/crystalline form, presumably because of the high cooling rates (typically more than  $10^6 \text{ K/s}$ ) occurring in such deposition processes upon impact of molten particles on the target material. For the coating W1, peaks from WC and  $\alpha\text{-W}_2\text{C}$  were recognized, and the C-deficient phases  $\text{W}_2\text{C}$  formed as a result of oxidation and decarburization during the coating deposition process. However, a distinct Co peak was not present in the coating in agreement with the results reported (Ref 11), which suggested that Co in WC/Co based thermal spray coatings was present as an amorphous phase. The XRD pattern of coating W2 is similar to that of the coating W1, but distinct WC and  $\alpha\text{-W}_2\text{C}$  peaks were not present; it may have formed because most of the original WC/12Ni particle was decarburized during the coating deposition process and the residual WC particles were in an amount that could not be detected by XRD.

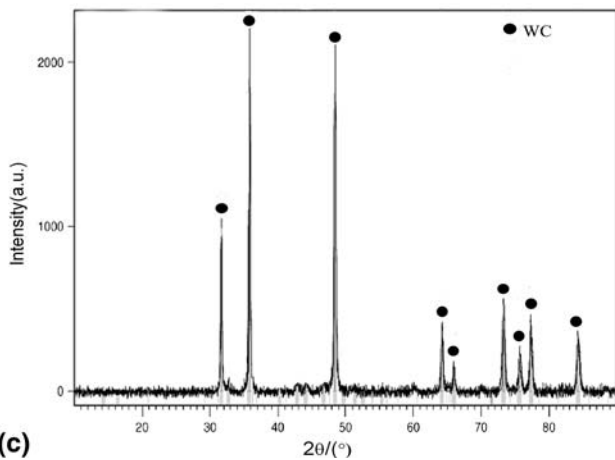
Figure 3 shows the cross-sectional microstructure of the as-sprayed coatings at the unetched condition. As indicated in Fig. 3, both coatings consist of flattened platelike lamellae oriented parallel to the substrate. Some pores were also present in the coatings. The measured porosity of the coatings W1 and W2 was 2.1% and 3.2%, respectively. Based on the analyzing results of microstructures and XRD patterns, the phases can be identified in both coatings, and the white metal matrix is Fe-Cr and the particles in a deeper gray contrast corresponds to  $\text{Fe}_2\text{B}$  hard phase, and the area in a dark contrast corresponds to pores. It is clear that a significant fraction of  $\text{Fe}_2\text{B}$  was distributed in the coating. However, it was confirmed that



(a)



(b)



(c)

**Fig. 1** XRD spectrum of feedstock powders used as fillers in cored wires. (a) FeB. (b) WC/12Co. (c) WC/12Ni

few carbides were recognized from the cross-sectional microstructure of the coatings. This possibly resulted from the fact that the substantial FeB particles were melted during spraying, while most WC particles were not melted and rebounded off after impact on the substrate.

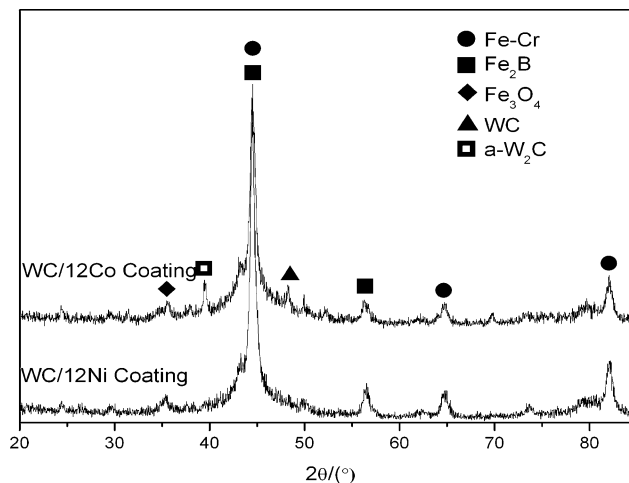


**Fig. 2** XRD spectrum of the as-sprayed coatings

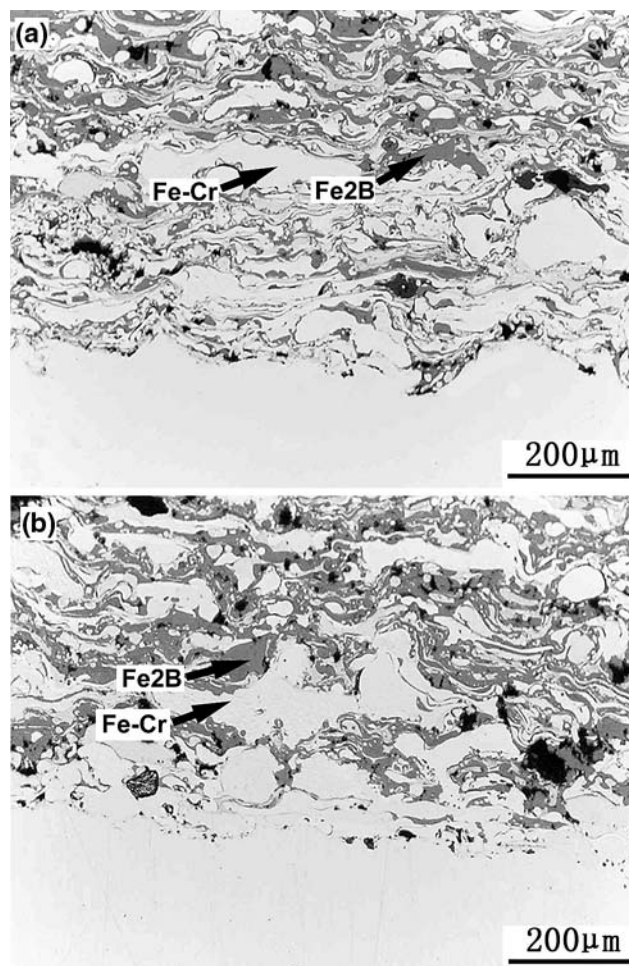


**Fig. 3** Cross-sectional microstructure of the as-sprayed coatings. (a) Coating W1. (b) Coating W2

Therefore, as-hard phases in the filler materials in the cored wire designed for arc spraying, FeB can be more easily retained in the coating than WC.



### 3.2 Wear Properties of Coatings

The hardness and relative wear resistance of the as-sprayed coatings are shown in Fig. 4. The microhardness values are the average of 10 measurements taken in the cross section of the coatings. Microhardness measurements on coatings yielded a value of 920 HV<sub>0.1</sub> for the coating W1 and 872 HV<sub>0.1</sub> for the coating W2. The average mass loss of the coating W1 was 0.1243 g, while the average mass loss of the coating W2 was 0.1794 g. As shown in Fig. 4, the coating W1 exhibited an excellent abrasive wear resistance that was 4.8 times higher than that of the arc sprayed 3Cr13 coating. Although the abrasive wear resistance of the coating W2 was not good as the coating W1, its wear resistance was still 3.3 times higher than that of the arc sprayed 3Cr13 coating.

Worn surface morphologies were examined under SEM to understand the wear behavior of the as-sprayed coatings. The locations for EDS analysis are shown in Fig. 5, and the contents of different elements at corresponding locations are shown in Table 2. As shown in Table 2, composition analysis of points A and B confirmed the inclusion of the primary carbide WC in the coatings.

The morphology of the abrasive worn surface of the as-sprayed coatings are shown in Fig. 5. As shown in Fig. 5(a), there are numerous plastic furrows on the worn surface of the 3Cr13 coating. It was believed to result from a typical microcutting mechanism. For the coating W1, some WC particles have come out in some regions of the coating surface (point A). It was suggested that the wear mechanism of the cermet coating was by selective removal of the binder caused probably by plastic deformation and fatigue due to the repeated action of the abrasive particles followed by the undermining of the carbide particles, resulting in their eventual pullout (Ref 12, 13). Fe-Cr metal matrix was softer than the WC and Fe<sub>2</sub>B hard phases and thus prone to plastic deformation. WC and Fe<sub>2</sub>B grains in the coating were held by the metallic phase. When the metallic phase was

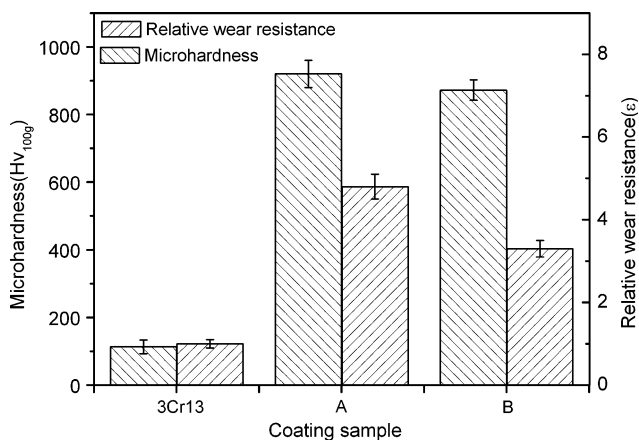


**Fig. 4** Microhardness and relative wear resistance of the as-sprayed coatings

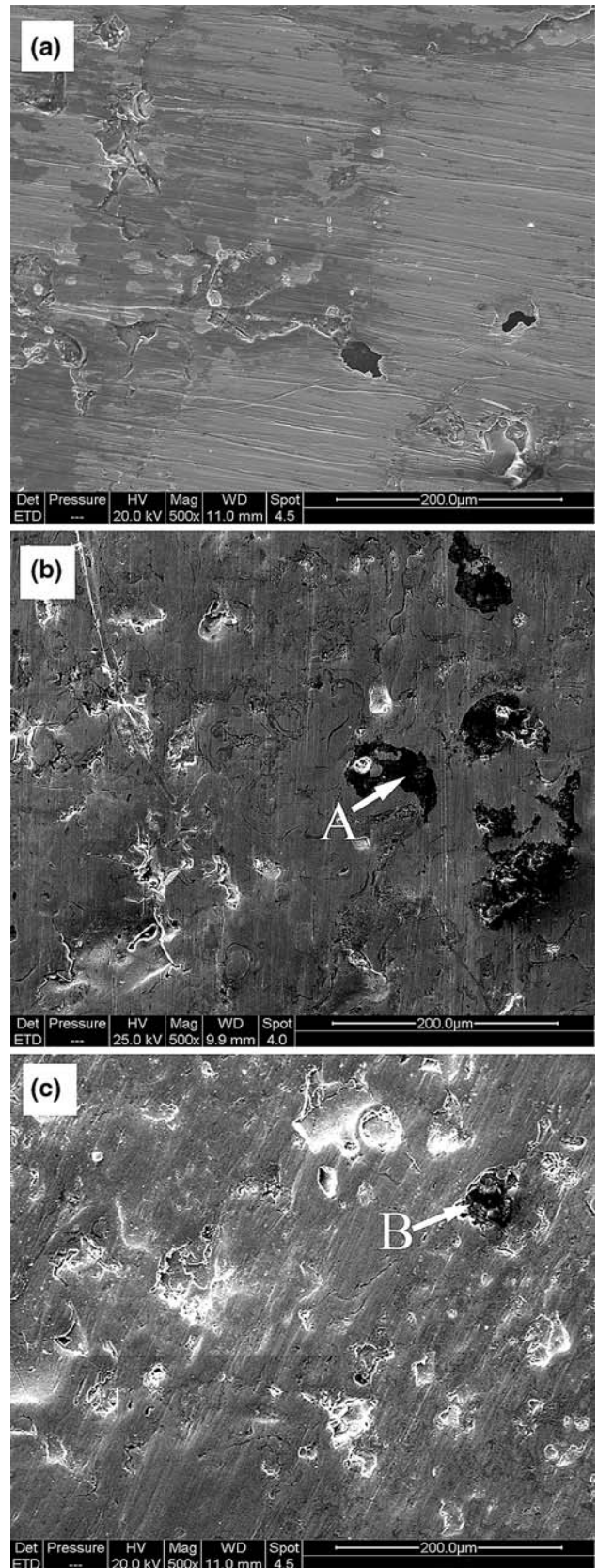


**Fig. 5** Worn surface morphologies of the as-sprayed coatings. (a) 3Cr13 coating. (b) Coating W1. (c) Coating W2

**Table 2 Composition of the different points in as-sprayed coatings**

Points	Element, wt. %				
	Fe	Cr	Ni	W	C
A	1.12	0.89	...	93.84	4.15
B	2.67	2.13	0.92	91.02	3.26

removed from the coating, the WC and Fe<sub>2</sub>B grains automatically come out. A similar type of grain removal has been reported elsewhere (Ref 12). For the coating W2, the mechanism of wear was similar with that of the coating W1. The high porosity and little carbide content may possibly be the reason for lower hardness and wear resistance. It was easier for cracks to initiate from defective regions such as pores than in a normal smooth surface; under the abrasion conditions, microcracks initiate and propagate along the interface between hard phase and the matrix. The propagation of cracks cause flaking off of the lamellae.

#### 4. Conclusions

The results of the present study on the arc sprayed Fe-FeB-WC coatings can be summarized:

- The coatings prepared by arc spraying using cored wires exhibited a typical lamellar structure. The majority of phases in both coatings were Fe-Cr and Fe<sub>2</sub>B. A trace of WC and  $\alpha$ -W<sub>2</sub>C was recognized from the XRD pattern of coating W1, but was not recognized in coating W2. The results indicated that it was easier to deposit an alloy-based coating containing FeB than one containing WC by arc spraying using cored wire with hard phase fillers.
- The average microhardnesses of two arc sprayed Fe-FeB-WC coatings were 920 HV<sub>0.1</sub> and 872 HV<sub>0.1</sub>, higher than that of an arc sprayed 3Cr13 coating. The coatings W1 with W2, coating W1 exhibited better abrasive wear resistance, which was 3.3 to 4.8 times than that of the 3Cr13 coating. The results

showed that a wear-resistant coating can be deposited by arc spraying using a cored wire of hard filler materials.

#### References

1. F. Rastegar and D.E. Richardson, Alternative to Chrome: HVOF Cermet C for High Horse Power Diesel Engines, *Surf. Coat. Technol.*, 1997, **90**(1-2), p 156-163
2. V. Stoica, R. Ahmed, and T. Itsukaichi, Influence of Heat-Treatment on the Sliding Wear of Thermal Spray Cermet Coatings, *Surf. Coat. Technol.*, 2005, **199**(1), p 7-21
3. P.K. Aw and B.H. Tan, Study of Microstructure, Phase and Microhardness Distribution of HVOF Sprayed Multi-Modal Structured and Conventional WC-17Co Coatings, *J. Mater. Process. Technol.*, 2006, **174**(1-3), p 305-311
4. Q. Yang, T. Senda, and A. Hirose, Sliding wear behavior of WC-12%Co coatings at elevated temperatures, *Surf. Coat. Technol.*, 2006, **200**(14-15), p 4208-4212
5. H.S. Sidhu, B.S. Sidhu, and S. Prakash, Mechanical and Microstructural Properties of HVOF Sprayed WC-Co and Cr<sub>3</sub>C<sub>2</sub>-NiCr Coatings on the Boiler Tube Steels Using LPG as the Fuel Gas, *J. Mater. Process. Technol.*, 2006, **171**(1), p 77-82
6. H. Du, C. Sun, W.G. Hua, T.G. Wang, J. Gong, X. Jiang, and S.W. Lee, Structure, Mechanical and Sliding Wear Properties of WC-Co/MoS<sub>2</sub>-Ni Coatings by Detonation Gun Spray, *Mater. Sci. Eng. A*, 2007, **445-446**, p 122-134
7. G.C. Ji, C.J. Li, Y.Y. Wang, and W.Y. Li, Microstructural Characterization and Abrasive Wear Performance of HVOF Sprayed Cr<sub>3</sub>C<sub>2</sub>-NiCr Coating, *Surf. Coat. Technol.*, 2006, **200**(24), p 6749-6757
8. Y. Ishikawa, S. Kuroda, J. Kawakita, Y. Sakamoto, and M. Takaya, Sliding Wear Properties of HVOF Sprayed WC-20%Cr3C2-7%Ni cermet coatings, *Surf. Coat. Technol.*, 2007, **201**, p 4718-4727
9. A.K. Maiti, N. Mukhopadhyay, and R. Raman, Effect of Adding WC Powder to the Feedstock of WC-Co-Cr Based HVOF Coating and Its Impact on Erosion and Abrasion Resistance, *Surf. Coat. Technol.*, 2007, **201**(18), p 7781-7788
10. T. Sahraoui, N.E. Fenineche, G. Montavon, and C. Coddet, Structure and Wear Behaviour of HVOF Sprayed Cr<sub>3</sub>C<sub>2</sub>-NiCr and WC-Co Coatings, *Mater. Des.*, 2003, **24**(5), p 309-313
11. S. Luyckx and C.N. Machio, Characterization of WC-VC-Co Thermal Spray Powders and Coatings, *Int. J. Refract. Met. Hard Mater.*, 2007, **25**(1), p 11-15
12. J.K.N. Murthy and B. Venkataraman, Abrasive Wear Behaviour of WC-CoCr and Cr3C2-20(NiCr) Deposited by HVOF and Detonation Spray Processes, *Surf. Coat. Technol.*, 2006, **200**(8), p 2642-2652
13. T. Sudaprasert, P.H. Shipway, and D.G. McCartney, Sliding Wear Behaviour of HVOF Sprayed WC-Co Coatings Deposited with Both Gas-Fuelled and Liquid-Fuelled Systems, *Wear*, 2003, **255**(7-12), p 943-949